ON THE CHARACTERIZATION AND APPLICATIONS OF A THREE-PARAMETER IMPROVED WEIBULL-WEIBULL DISTRIBUTION

A. S. Mohammed[1] , B. Abba[2,3*], I. Abdullahi[2], Y. Zakari[1], A. I. Ishaq[1]

[1]Department of Statistics, Ahmadu Bello University, Zaria.
[2]Department of Mathematics, Yusuf Maitama Sule University, Kano-Nigeria.
[3]School of Mathematics and Statistics, Central South University, Changsha, Hunan Province, China.
mohammedas@abu.edu.ng
badamasiabba@gmail.com
ibraabdul@googlemail.com
yzakari@abu.edu.ng
binishaq05@gmail.com
*Corresponding author: Email: babba@yumsuk.edu.ng

Abstract

Parametric modeling of complex lifetime data characterized with nonmonotone hazard rate (NMHR) has in recent years attract the interest of many researchers and practitioners. The three-parameter improved Weibull-Weibull distribution introduced in 2022 has demonstrated a better NMHR modeling potential in the analysis of several failure times identified with bathtub hazard rate (BHR). In this study, we present the characterization, properties and two data sets' applications of the distribution. Various properties of the distribution obtained, include moment generating function, moments, skewness, kurtosis, and some types of entropy. Numerical results for mean, variance, skewness, and kurtosis are computed using simulation studies. Estimation of the distribution parameters is performed using the method of maximum likelihood, and the estimation method is assessed by Monte Carlo simulation experiments. The two illustrations further ascertain the capability of the model for modeling lifetime data from different scientific investigation areas.

Keywords: Improved Weibull-Weibull distribution, non-monotone failure rate, characterization, maximum likelihood method, failure time data.

1. Introduction

Weibull distribution is one of the leading and widely used classical distributions. It has played a vital role in solving many problems in applied areas, such as reliability engineering, renewable energy, weather forecast, and biological studies analysis. For example, the Weibull model is used in modelling the failure time of devices [1], analysis of wind speed data to determine the wind power density [2], furthermore,[3] applied the distribution to describe soil particle-size and was recently used for fatigue life prediction of mechanical parts [4]. Because of its positively and negatively skewed density shapes, the distribution may be the first choice when modeling monotone hazard rates. One drawback with Weibull is its inability to accommodate non-monotone failure rates, such as the bathtub and unimodal failure rates [5]. For instance, the unimodal-shaped failure rate can be observed in the course of a successful surgery, where the patient is at high risk initially due to infection and other complications. The bathtub-shaped failure rate can be observed

in the course of a population followed from birth or manufactured items with early failure due to faulty parts. Different new classes of distributions were developed based on modifications of the Weibull distribution to cope with the non-monotonic failure rates. Among others, are the exponentiated Weibull by [6], modified Weibull by [7], odd Weibull by [8], beta modified Weibull by [9], Weibull-Weibull by [10], Weibull-exponential by [11], odd generalized exponential-Weibull by [12], new Weibull-Weibull by [13], exponentiated additive Weibull distribution by [14], on monotonic and non-monotonic failure rates by [15], Four-Parameter Weibull distribution by [16] and flexible additive Chen-Gompertz by [17]. These distributions have one or more additional parameter(s) compared to Weibull distribution that makes them more flexible for modeling datasets with both monotone and non-monotone failure rates. The improved Weibull-Weibull (IWW3) distribution is a three-parameter model recently established by [18]. The distribution was proposed as an enhanced version of Weibull-Weibull (WW) distribution by [10] introduced in an earlier study to widen its applicability in modeling different complex lifetime data distinguished by various monotone and non-monotone hazard rate (HR) shapes. The IWW3 distribution is expressed by the following survival/reliability function as;

$$S(x) = \exp\left\{-\int_0^{\infty} h(t)\mathrm{d}x\right\} = \exp\left\{-\left(e^{\zeta^{\eta}} - 1\right)^{\varphi}\right\}, \quad t > 0, \tag{1}$$

where $\zeta = \frac{x}{\tau}$, $\eta > 0$ and $\varphi > 0$ are the two shape parameters, $\tau > 0$ is the scale parameter of the model, and $h(x)$ represents the associated HR function (HRF) of the model, defined as

$$h(x) = \frac{\eta\varphi}{\tau}\zeta^{\eta-1}e^{\zeta^{\eta}}\left(e^{\zeta^{\eta}} - 1\right)^{\varphi-1}. \tag{2}$$

The HRF of IWW3 distribution was characterized to have an increasing shape when $\varphi, \eta \geq 1$, and a decreasing pattern when $\varphi, \eta < 1$. Depending on the chosen values within the ranges of $\eta > 1$ and $\varphi\eta < 1$, the HRF exhibits various bathtub curves. The HRF shapes are displayed in Figure 1, which visually explains the three main forms of the HFR shapes.

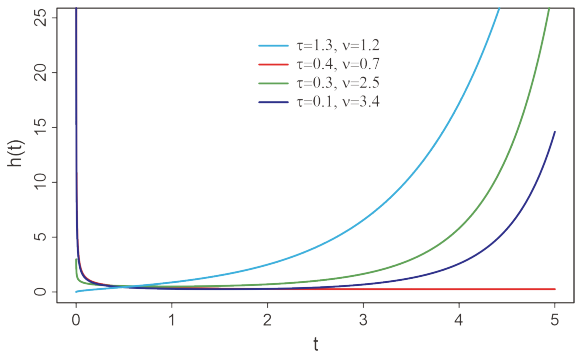

Figure 1: *Curves describing various shapes of IWW3 hazard rate function at different values.*

The probability density function (PDF) of the model is expressed as

$$f(x) = \frac{\eta\varphi}{\tau}\zeta^{\eta-1}e^{\zeta^{\eta}}\left(e^{\zeta^{\eta}} - 1\right)^{\varphi-1}\exp\left[-\left(e^{\zeta^{\eta}} - 1\right)^{\varphi}\right]. \tag{3}$$

The distribution was demonstrated to provide a better fit in practice among several other two to five-parameter Weibull and non-Weibull distributions. More specifically, the censored failure and running times of 30 devices by[19] was identified to exhibit bathtub-shaped HR. The findings established the superiority of IWW3 distribution over some well-known Weibull extensions, including the exponentiated Weibull by [6], modified Weibull by [7], exponential Weibull by [20], alongside the WW [10] and other distributions. Motivated by the IWW3 distribution flexibility, and the original study by [18] only proposed the model, discussed its failure rate function and estimation methods. In this study, we present other important aspects of the

distribution, including the model's characterizations and some of its properties. Other real-life data applications of the distributions are also demonstrated.

The rest of the paper is arranged as follows. Section 2 discuss some of the properties and entropies of the distribution. The characterization of the distribution by two truncated moments and based on hazard function are given in section 3. The estimation of the proposed distribution parameters via the maximum likelihood method is presented in section 4. In sections 5 and 6, we assessed the estimators numerically by simulation studies and applications of the model to two lifetime data, respectively. We conclude the paper in section 7.

2. Distribution properties

Here, we discuss the moment generating function, moments, Rényi entropy and Mathai-Houbold entropy. We obtained an approximation for the values of the mean, variance, skewness and kurtosis of X using Monte Carlo simulation technique.

2.1. Moment generating function and moments

Definition 1: Let X be a random variable with the IWW3 density function (3). Then the moment generating function of X is given by

$$M_X(s) = \varphi \sum_{i\geq 0}\sum_{j\geq 0} \frac{(-1)^{i+j}\Gamma(\varphi(i+1))}{i!j!\Gamma(\varphi(i+1)-j)} \sum_{p\geq 0} \frac{\tau^p s^p \Gamma(1+p/\eta)}{p!\,(j-\varphi(i+1))^{1+\frac{p}{\eta}}} \tag{4}$$

The r^{th} moment about origin of X is generated from (4) , and is define as follows.

Definition 2: Let X be a random variable with the IWW3 density function (3). Then the r^{th} ($r > 0$, real) generalized ordinary moment of X is $\mu_r = \int_{-\infty}^{\infty} x^r f(x)\,dx$. For $X \sim$IWW3 (η, φ, τ), the r^{th} moment from (4), is given as

$$\mu_r = E(X^r) = \sum_{i\geq 0}\sum_{j\geq 0} \frac{(-1)^{i+j}\Gamma(\varphi(i+1))\,\Gamma(1+r/\eta)\,\tau^r\varphi}{i!j!(j-\varphi(i+1))^{1+r/\eta}\Gamma(\varphi(i+1)-j)}, \qquad r \in N \tag{5}$$

In particular , the first four moments (for $r = 1, \ldots, 4$) can be used to calculate the mean (μ_1), variance (σ^2), skewness ($\sqrt{\beta_1}$) and kurtosis (β_2) based on some well-known results.
The Monte Carlo simulation was performed for $N = 1000$ samples each of size $n = 200$ from the IWW3$(\eta,\ \varphi,\ \tau)$ distribution, with $\Psi = (\eta_0,\ \varphi_0,\ 1.5\ )^T$ - the vector of parameters, where $\eta = 0.7,\ 0.9,\ 1.5,\ 2.0$ and 3.0, and $\varphi = 0.5,\ 1.0,\ 1.5,\ 2.0$ and 3.0. Table 1 listed the numerical results for the mean, variance, skewness and kurtosis with their standard deviations (SDs) in parenthesis. We can notice From the Table, that the estimates of these properties varies for various combinations of the distribution parameters with a consistent decrease in the SDs for the mean and variance. The distribution shifted from right to left-skewed distribution when $\eta\varphi \geq 2$. The skewness and kurtosis plots are displays in Figure 2 as a functions of η and φ. A decrease in the values of the skewness and kurtosis are observed from the plots as values of the η and φ increases.

2.2. Rényi and Mathai-Houbold entropies

Definition 3: Let the random variable X have the density function given by (3). Then the Rényi entropy of X is given by

$$I_T(\alpha) = \frac{1}{1-\alpha}\log\left(M_{i,j}(\alpha,\Psi)\ \right) \tag{6}$$

where, $M_{i,j}(\alpha,\Psi) = \frac{\eta^{\alpha-1}\varphi}{\tau^{\alpha-1}} \sum_{i\geq 0}\sum_{j\geq 0} \frac{(-1)^{i+j}\Gamma(\varphi(i+1)-(\alpha-1))\Gamma\left((\eta-1)(\alpha-1)\eta^{-1}+1\ \right)}{i!j!(j-\varphi(i+1))^{(\eta-1)(\alpha-1)\eta^{-1}+1}\ \Gamma(\varphi(i+1)-(\alpha+j-1))}$, $\alpha > 0$ *and* $\alpha \neq 1$.

Table 1: *Mean, variance, skewness and kurtosis with standard deviations between parentheses; $\tau = 1.5$ and some values of η and φ.*

η	φ	**Mean** (μ_1')	**Variance** (σ^2)	**Skewness**$(\sqrt{\beta_1})$	**Kurtosis**(β_2)
	0.5	1.195 (0.128)	3.021 (0.635)	2.045 (0.408)	7.729 (3.268)
	1.0	0.830 (0.057)	0.609 (0.091)	1.277 (0.273)	4.563 (1.598)
0.7	1.5	0.778 (0.038)	0.284 (0.033)	0.785 (0.197)	3.264 (0.833)
	2.0	0.772 (0.030)	0.173 (0.018)	0.466 (0.163)	2.784 (0.510)
	3.0	0.785 (0.021)	0.089 (0.008)	0.074 (0.143)	2.617 (0.275)
	0.5	1.066 (0.094)	1.660 (0.263)	1.535 (0.257)	5.099 (1.506)
	1.0	0.875 (0.048)	0.450 (0.053)	0.870 (0.186)	3.295 (0.774)
0.9	1.5	0.862 (0.034)	0.229 (0.022)	0.451 (0.151)	2.690 (0.439)
	2.0	0.871 (0.027)	0.144 (0.013)	0.177 (0.139)	2.560 (0.293)
	3.0	0.894 (0.019)	0.075 (0.007)	-0.160 (0.142)	2.711 (0.227)
	0.5	1.007 (0.061)	0.710 (0.071)	0.780 (0.139)	2.736 (0.400)
	1.0	1.001 (0.036)	0.259 (0.022)	0.231 (0.122)	2.376 (0.231)
1.5	1.5	1.030 (0.027)	0.140 (0.013)	-0.096 (0.127)	2.524 (0.190)
	2.0	1.054 (0.021)	0.088 (0.009)	-0.304 (0.139)	2.782 (0.234)
	3.0	1.086 (0.015)	0.045 (0.005)	-0.546 (0.164)	3.246 (0.372)
	0.5	1.032 (0.050)	0.492 (0.041)	0.448 (0.116)	2.238 (0.217)
	1.0	1.077 (0.031)	0.188 (0.016)	-0.062 (0.116)	2.376 (0.162)
2.0	1.5	1.116 (0.022)	0.101 (0.010)	-0.349 (0.135)	2.766 (0.232)
	2.0	1.142 (0.018)	0.063 (0.007)	-0.522 (0.154)	3.126 (0.334)
	3.0	1.173 (0.012)	0.031 (0.004)	-0.711 (0.182)	3.624 (0.500)
	0.5	1.098 (0.039)	0.305 (0.023)	0.041 (0.104)	2.064 (0.117)
	1.0	1.178 (0.024)	0.115 (0.011)	-0.416 (0.127)	2.728 (0.231)
3.0	1.5	1.219 (0.017)	0.059 (0.007)	-0.646 (0.158)	3.306 (0.392)
	2.0	1.243 (0.013)	0.036 (0.004)	-0.772 (0.180)	3.702 (0.521)
	3.0	1.269 (0.009)	0.017 (0.002)	-0.895 (0.206)	4.140 (0.683)

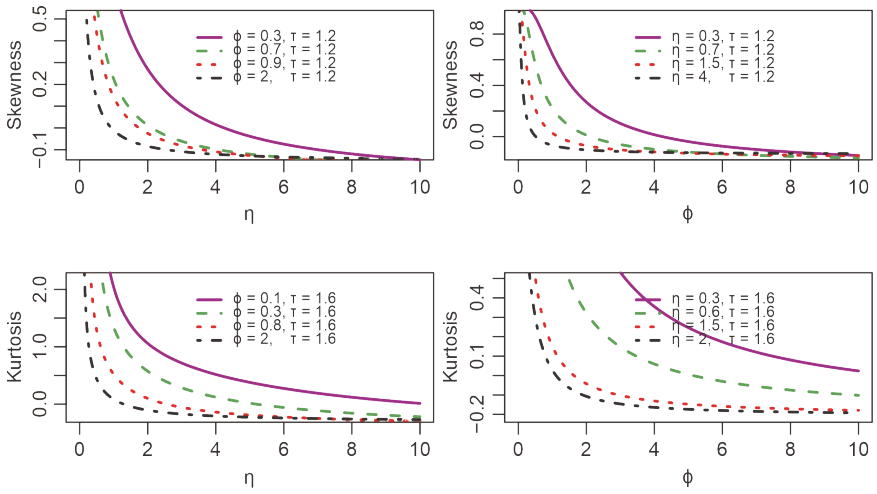

Figure 2: *Plots of the Skewness and Kurtosis of the IWW3 as a function of η and φ, respectively.*

Definition 4: Let X have the PDF given by (3). Then the Mathai-Houbold (M-H) entropy of X is given by

$$J_{MH}(\delta) = \frac{\left(\frac{\eta}{\tau}\right)^{1-\delta} \varphi^{2-\delta} M_{i,j}^{*}(\delta, \Psi) - 1}{\delta - 1} \tag{7}$$

wher e, $M^{*}_{i,j}(\delta,\Psi) = \sum_{i\geq 0}\sum_{j\geq 0}\frac{(-1)^{i+j}(2-\delta)^{i}\Gamma(\varphi(2-\delta+i)-(1-\delta))\Gamma\left((2-\delta)-(1-\delta)\eta^{-1}\right)}{i!j!(j-\varphi(2-\delta+i))^{(2-\delta)-(1-\delta)\eta^{-1}}\ \Gamma(\varphi(2-\delta+i)-(1-\delta+j))}$, $\delta \neq 1$ and $\delta < 2$.

We presented some numerical values for the Rényi and Mathai-Houbold entropies in Table 2. We note a decrease in the entropy as the values of either η or φ increases for the Rényi. While for the M-H, we observed that the entropy increases with an increase in η and decreases with an increase in φ. It can further be seen that entropy can take negative values, which may be understood as a loss of information in physical systems [21].

Table 2: *Rényi and Mathai-Houbold entropies for some values of the parameters*

$\eta\ \downarrow$	φ	τ	α	Rényi	$\varphi\ \downarrow$	η	τ	α	Rényi
0.1				2.9245	0.7				1.1692
0.2				1.2632	0.9				0.9486
0.4				0.8462	1.2				0.7302
0.6	1.1	1.2	0.6	0.7562	1.4	0.5	1.2	0.6	0.6229
0.7				0.7243	1.6				0.5330
0.8				0.6940	1.8				0.4549
0.85				0.6790	2.0				0.3853
	φ	τ	δ	M-H		η	τ	δ	M-H
0.58				0.3928	0.68				2.0974
0.60				0.6530	0.70				1.4760
0.62				0.8740	0.72				0.9609
0.64	0.7	1.2	0.6	1.0635	0.74	0.5	1.2	1.6	0.5311
0.66				1.2278	0.76				0.1700
0.68				1.3716	0.78				-0.1352
0.70				1.4986	0.80				-0.3946

3. Characterization

Characterization guides an investigator in designing a stochastic model for a particular modelling problem to know if the model fits the conditions of a specific underlying probability distribution. The investigator will depend on the characterization of the chosen distribution. The technique characterizes distribution and its random variable when the distribution conditions are similar to those of the random variable. This section presents the IWW3 distribution characterization in two directions (i) in terms of the simple relationship for the ratio of two truncated moments and (ii) based on the hazard function. We employed a theorem due to [22], for the first characterization (see Theorem 1). Note that the first characterization can be utilized even when the CDF's closed-form does not exist.

3.1. Characterizations based on two truncated moments

Theorem 1. Let (Ω,Σ,P) be a given probability space and let $H=[a_1,a_2]$, - be an interval for some $a_1 < a_2$ ($a_1=-\infty, a_2=\infty$ might as well be allowed). Let $X:\Omega\longrightarrow H$ be a continuous random variable with the distribution function F and let q_1 and q_2 be two real functions defined on H such that

$E[q_2(X)|X\geq x] = E[q_1(X)|X\geq x]\,\eta(x), x\in H$

is defined with some real function η. Assume that $q_1, q_2\in C^1(H), \eta\in C^2(H)$ and F is twice continuously differentiable and strictly monotone function on the set . Finally, assume that the equation $\eta q_1 = q_2$ has no real solution in the interior of H. Then F is uniquely determined by the functions q_1, q_2 and η , particularly

$$F(x) = \int_a^x c\left|\frac{\eta'(u)}{\eta(u)q_1(u)-q_2(u)}\right|\exp\left[-s(u)\right]du$$

where the function s is a solution of the differential equation $s' = \frac{\eta' q_1}{\eta q_1 - q_2}$ and C is a constant chosen to make $\int_H dF = 1$.

Proposition 1: Let $X : \Omega \longrightarrow (0, \infty)$ be a continuous random variable and let $q_1(x) = 1$ and $q_2(x) = \exp[-\kappa^{\varphi}]$, where $\kappa = e^{(x/\tau)^{\eta}} - 1$ and $x > 0$. The random variable X has PDF (3), if and only if the function $\eta(x)$ defined in Theorem 1 has the form

$$\eta(x) = \frac{1}{2}\exp[-\kappa^{\varphi}], \qquad x > 0.$$

Proof. Let the random variable X has the PDF (3), then

$$(1 - F(x))E[q_1(X)|X \geq x] = \exp[-\kappa^{\varphi}], \qquad x > 0,$$

and

$$(1 - F(x))E[q_2(X)|X \geq x] = \frac{1}{2}\exp[-\kappa^{\varphi}], \qquad x > 0.$$

Further,

$$\eta(x)q_1(x) - q_2(x) = -\frac{1}{2}\exp[-\kappa^{\varphi}] < 0, \qquad \text{for } x > 0$$

Conversely, if η is given as above, then

$$s'(x) = \frac{\eta'(x)q_1(x)}{\eta(x)q_1(x) - q_2(x)} = \frac{\eta\varphi}{\tau}(x/\tau)^{\eta-1}(\kappa+1)\kappa^{\varphi-1} = \frac{f(x)}{\bar{F}(x)}, \qquad \text{for } x > 0$$

Therefore, according to Theorem 1, X has PDF (3).

Corollary 1. Let $X : \Omega \longrightarrow (0, \infty)$ be a continuous random variable and let $q_1(x)$ be as in Proposition 1. The PDF of X is (3) if and only if there exist functions $q_2(x)$ and $\eta(x)$ defined in Theorem 1 satisfying the differential equation

$$\frac{\eta'(x)q_1(x)}{\eta(x)q_1(x) - q_2(x)} = \frac{\eta\varphi}{\tau}(x/\tau)^{\eta-1}(\kappa+1)\kappa^{\varphi-1}, \qquad \text{where } \kappa = e^{(x/\tau)^{\eta}} - 1 \text{ and } x > 0$$

Remark 1. The general solution of the differential equation in Corollary 1 is

$$\eta(x) = \exp[-\kappa^{\varphi}]\left[-\int_0^{\infty}\frac{\eta\varphi}{\tau}(x/\tau)^{\eta-1}(\kappa+1)\kappa^{\varphi-1}\exp[-\kappa^{\varphi}](q_1)^{-1}q_2 dx + D\right]$$

where D is a constant. Note that one set of functions satisfying the differential equation is given in Proposition 1 with $D = 0$.

3.2. Characterization based on hazard function

The hazard function, $h(x)$ of a twice differentiable distribution function, $F(x)$, satisfy the following first order differential equation

$$\frac{f'(x)}{f(x)} = \frac{h'(x)}{h(x)} - h(x) \tag{8}$$

Proposition 2: Let $X : \Omega \longrightarrow (0, \infty)$ be a continuous random variable. The random variable X has PDF (3), if and only if its hazard function $h(x)$ satisfy the following differential equation

$$h'(x) - \left\{\frac{\eta}{\tau}(x/\tau)^{(\eta-1)} + \frac{(\eta-1)}{\tau}(x/\tau)^{(-1)}\right\}h(x) = \frac{\eta^2(\varphi-1)}{\tau^2}(x/\tau)^{2(\eta-1)}(\kappa+1)^2 \times \kappa^{\varphi-2}$$

under the boundary conditions $h(0) \geq 0$ and $\kappa = e^{(x/\tau)^{\eta}} - 1$.

Proof. If random variable X has the hazard function given in (2), then

$$h'(x) = \frac{\eta^2(\varphi-1)}{\tau^2}(x/\tau)^{2(\eta-1)}(\kappa+1)^2\kappa^{\varphi-2} + \frac{\eta^2\varphi}{\tau^2}(x/\tau)^{2(\eta-1)}(\kappa+1)\kappa^{\varphi-1} + \frac{\eta(\eta-1)\varphi}{\tau^2}(x/\tau)^{(\eta-2)}(\kappa+1)\kappa^{\varphi-1}$$

and hence,

$$\begin{aligned}\frac{h'(x)}{h(x)} - h(x) =& \frac{\eta(\varphi-1)}{\tau}(x/\tau)^{(\eta-1)}(\kappa+1)\kappa^{-1} + \frac{\eta}{\tau}(x/\tau)^{(\eta-1)} + \frac{(\eta-1)}{\tau}(x/\tau)^{(-1)} \\ & - \frac{\eta}{\tau}(x/\tau)^{(\eta-1)}(\kappa+1)\kappa^{\varphi-1}\end{aligned} \tag{9}$$

Similarly ,

$$\begin{aligned}f'(x) =& f(x)\left\{\frac{\eta(\varphi-1)}{\tau}(x/\tau)^{(\eta-1)}(\kappa+1)\kappa^{-1} + \frac{\eta}{\tau}(x/\tau)^{(\eta-1)} + \frac{(\eta-1)}{\tau}(x/\tau)^{(-1)}\right\} \\ & - \frac{\eta\varphi}{\tau}(x/\tau)^{(\eta-1)}(\kappa+1)\kappa^{\varphi-1}f(x)\end{aligned}$$

and thus,

$$\begin{aligned}\frac{f'(x)}{f(x)} =& \frac{\eta(\varphi-1)}{\tau}(x/\tau)^{(\eta-1)}(\kappa+1)\kappa^{-1} + \frac{\eta}{\tau}(x/\tau)^{(\eta-1)} + \frac{(\eta-1)}{\tau}(x/\tau)^{(-1)} \\ & - \frac{\eta\varphi}{\tau}(x/\tau)^{(\eta-1)}(\kappa+1)\kappa^{\varphi-1}\end{aligned} \tag{10}$$

Equations (9) and (10) satisfied the differential equation (8), and hence, the IWW3 random variable X has the hazar d function (2).

4. Parameter estimation

In this section, we use the method of maximum likelihood to estimate the unkno wn parameters of the distribution for complete dataset. Let $x_1, x_2, \ldots, x_n$ be a random sample of size n from the IWW3 model with the vector of parameters $\Psi = (\eta, \varphi, \tau)$. Then the log-likelihood function of Ψ from the PDF (3) is

$$\begin{aligned}\ell(\Psi) =& n\log\left(\frac{\eta\varphi}{\tau}\right) + (\eta-1)\sum_{i=1}^{n}\log(z_i) + \varphi\sum_{i=1}^{n}z_i^{\eta} + (\varphi-1)\sum_{i=1}^{n}\log\left(1-e^{-z_i^{\eta}}\right) \\ & - \sum_{i=1}^{n}\left(e^{z_i^{\eta}}-1\right)^{\varphi}\end{aligned}$$

wher e, $z_i = \frac{x_i}{\tau}$. The estimate $\widehat{\Psi} = (\widehat{\eta}, \widehat{\varphi}, \widehat{\tau})^T$ of $\Psi = (\eta, \varphi, \tau)^T$ is deter mined by maximizing the log-likelihood function $\ell(\Psi)$ with respect to each of the IWW3 parameters. Thus, we have follo wing scor e functions.

$$\begin{aligned}\frac{\partial\ell(\Psi)}{\partial\eta} =& \frac{n}{\eta} + \sum_{i=1}^{n}\log z_i - \varphi\sum_{i=1}^{n}\left(e^{z_i^{\eta}}-1\right)^{\varphi-1}e^{z_i^{\eta}}z_i^{\eta}\log(\tau z_i) + \varphi\sum_{i=1}^{n}z_i^{\eta}\log(\tau z_i) \\ & + (\varphi-1)\sum_{i=1}^{n}z_i^{\eta}\log(\tau z_i)\left(e^{z_i^{\eta}}-1\right)^{-1}\end{aligned} \tag{11}$$

$$\frac{\partial\ell(\Psi)}{\partial\varphi} = \frac{n}{\varphi} - \sum_{i=1}^{n}\left(e^{z_i^{\eta}}-1\right)^{\varphi}\log\left(e^{z_i^{\eta}}-1\right) + \sum_{i=1}^{n}z_i^{\eta} + \sum_{i=1}^{n}\log\left(1-e^{-z_i^{\eta}}\right) \tag{12}$$

and

$$\frac{\partial\ell(\Psi)}{\partial\tau} = -\frac{\eta}{\tau}\left[n + \varphi\sum_{i=1}^{n}z_i^{\eta}\left(1-e^{z_i^{\eta}}\left(e^{z_i^{\eta}}-1\right)^{\varphi-1}\right) - (\varphi-1)\sum_{i=1}^{n}z_i^{\eta}\left(e^{z_i^{\eta}}-1\right)^{-1}\right] \tag{13}$$

Solving equations (11)-(13) analytically may be intractable. Thus, a numerical appr oach is adopted to obtain the maximum likelihood estimates (MLEs) of the parameters $\Psi = (\eta, \varphi, \tau)^T$ with a good set of initial values using R statistical package. To obtain the asymptotic inter val estimation of

$\Psi = (\eta, \varphi, \tau)$, we deter mine the obser ved Fisher infor mation matrix. The 3×3 Fisher infor mation matrix is

$$J(\Psi) = -\begin{pmatrix} J_{\eta\eta}(\Psi) & J_{\eta\varphi}(\Psi) & J_{\eta\tau}(\Psi) \\ J_{\varphi\eta}(\Psi) & J_{\varphi\varphi}(\Psi) & J_{\varphi}(\Psi) \\ J_{\tau\eta}(\Psi) & J_{\tau\varphi}(\Psi) & J_{\tau\tau}(\Psi) \end{pmatrix}$$

wher e the expr essions of $J_{\Psi_i,\Psi_j} = \frac{\partial^2 \ell(\Psi)}{\partial \Psi_i \partial \Psi_j}$, $i, j = 1, 2, 3$. Thus, the appr oximate variance of $\Psi = (\eta, \varphi, \tau)$ can be obtain as

$$J^{-1}(\hat{\Psi}) = \begin{pmatrix} var(\hat{\eta}) & cov(\hat{\eta}, \hat{\varphi}) & cov(\hat{\eta}, \hat{\tau}) \\ cov(\hat{\varphi}, \hat{\eta}) & var(\hat{\varphi}) & cov(\hat{\varphi}, \hat{\tau}) \\ cov(\hat{\tau}, \hat{\eta}) & cov(\hat{\tau}, \hat{\varphi}) & var(\hat{\tau}) \end{pmatrix}$$

Hence, the $100(1-\alpha)\%$ asymptotic confidence inter vals of $\Psi = (\eta, \varphi, \tau)$ are giv en by $\hat{\eta} \pm Z_{\frac{\alpha}{2}}\sqrt{var(\hat{\eta})}$, $\hat{\varphi} \pm Z_{\frac{\alpha}{2}}\sqrt{var(\hat{\varphi})}$, and $\hat{\tau} \pm Z_{\frac{\alpha}{2}} var(\hat{\tau})$.

wher e Z_α is the upper α^{th} per centile of the standar d nor mal distribution.

5. Simulation results

The main objectiv e in this section is to evaluate the perfor mance of the maximum likelihood method for estimating the IWW3 distribution parameters for a complete dataset via Monte Carlo simulation. For this pur pose, we used six diffe rent combinations of the distribution parameters, including (1.8, 0.5, 0.5), (1.8, 0.7, 0.5), (1.8, 0.9, 0.5), (2, 0.5, 0.5), (2, 0.7, 0.5), and (2, 0.9, 0.5). The pr ocess is repeated 1000 times for four sample size s n = 100, 150, 200, and 300. Table 3 pr esents the MLEs, Biases, and Mean Squar e Errors (MSEs) of the parameters. Based on the results, we obser ve that the ML method perfor ms w ell for estimating the distribution parameters. Also, as the sample size incr eases, the biases and the MSEs of the MLEs decr eases as expected.

6. Applications

In this section, we analyze tw o diffe rent datasets to assess the potentiality of the IWW3 distribution in practice. The datasets are Aarset data [23] and Meeka and Escoba data [19]. Both the tw o datasets hav e a bathtub-shaped hazar d rate. We compar ed the results of the IWW3(Ψ) with Weibull and other Weibull extended models, including the exponentiated Weibull (EW) by [6], Weibull-W eibull(WW) by [10], Weibull-exponential (WE) by [11] and new Weibull-W eibull (NW-W) by [13]. To accomplish the pur pose, We manage the maximum $\ell(\hat{\Psi})$,Akaike Infor mation Criterion (AIC), Consistent Akaike Infor mation Criterion (CAIC) and Bayesian Infor mation Criterion (BIC). The Kolmogor ov-Smir nov (K-S) test is used to measur e the closeness betw een the em pirical and the fitted distribution.Generally , the smaller the value of these statistics, the better the model fit the dataset. All computations were done using RStudio 1.2.5042 softw are.

6.1. Aarset data

Her e, we emplo yed Aarset data [23], which is consider ed by many authors, such as [6], as standar d data for assessing distributions with bathtub-shaped FR. It repr esents the failur e times of fifty components placed on life test at time zer o. The data revealed a bathtub-shaped FR, as sho wn by the TTT-plot in Figur e 3. Table 4 pr esents the MLEs of the parameters of IWW3(Ψ) together with that of EW, WE, W, WW, and NW-W for the Aarset data. From Table 5, the IWW3(Ψ) has the smallest $-\ell(\hat{\Psi})$, AIC, CAIC, and BIC values, thus, the IWW3 model pr ovide a best fit for the Aarset data. For the non-parametric goodness-of-fit statistics, the IWW3 m odel has the smallest K-S value with the highest p-v alue, which suggests that the IWW3 model has a better fit for the data set than the other competing models.

Table 3: *MLEs, Biases, and MSEs of the distribution parameters.*

			Estimates			Biases			MSEs		
n	η	φ	$\hat{\eta}$	$\hat{\varphi}$	$\hat{\tau}$	$\hat{\eta}$	$\hat{\varphi}$	$\hat{\tau}$	$\hat{\eta}$	$\hat{\varphi}$	$\hat{\tau}$
100	1.8	0.5	1.9714	0.5414	0.5263	0.1714	0.0414	0.0263	0.4260	0.1539	0.1529
	1.8	0.7	2.0089	0.9619	0.6985	0.2089	0.2619	0.1985	0.7313	2.2978	2.2686
	1.8	0.9	2.0485	1.5201	0.8309	0.2485	0.6201	0.3309	1.1138	3.2315	2.9566
	2.0	0.5	2.1910	0.5405	0.5189	0.1910	0.0405	0.0189	0.5269	0.0671	0.0658
	2.0	0.7	2.2326	0.9666	0.6548	0.2326	0.2666	0.1548	0.9076	1.3555	1.3084
	2.0	0.9	2.2756	1.5279	0.7601	0.2756	0.6279	0.2601	1.3719	2.1311	1.8045
150	1.8	0.5	1.9050	0.5146	0.5039	0.1050	0.0146	0.0039	0.2569	0.0013	0.0011
	1.8	0.7	1.9312	0.7964	0.5378	0.1312	0.0964	0.0378	0.4453	0.2475	0.2397
	1.8	0.9	1.9570	1.1864	0.6115	0.1570	0.2864	0.1115	0.6846	0.7578	0.6882
	2.0	0.5	2.1184	0.5147	0.5037	0.1184	0.0147	0.0036	0.3217	0.0012	0.0010
	2.0	0.7	2.1458	0.7968	0.5304	0.1458	0.0968	0.0304	0.5492	0.1516	0.1431
	2.0	0.9	2.1742	1.1878	0.5875	0.1742	0.2878	0.0875	0.8443	0.4836	0.4085
200	1.8	0.5	1.8735	0.5085	0.5027	0.0735	0.0085	0.0027	0.1610	0.0007	0.0006
	1.8	0.7	1.8896	0.7463	0.5112	0.0896	0.0463	0.0112	0.2781	0.0263	0.0243
	1.8	0.9	1.9039	1.0521	0.5388	0.1039	0.1521	0.0388	0.4310	0.1530	0.1314
	2.0	0.5	2.0825	0.5083	0.5024	0.0825	0.0083	0.0024	0.1995	0.0006	0.0005
	2.0	0.7	2.1005	0.7456	0.5090	0.1005	0.0456	0.0090	0.3430	0.0145	0.0125
	2.0	0.9	2.1154	1.0523	0.5315	0.1154	0.1523	0.0315	0.5321	0.1015	0.0793
300	1.8	0.5	1.8509	0.5050	0.5018	0.0509	0.0050	0.0018	0.1077	0.0004	0.0004
	1.8	0.7	1.8621	0.7222	0.5037	0.0621	0.0222	0.0037	0.1887	0.0011	0.0006
	1.8	0.9	1.8712	0.9718	0.5136	0.0712	0.0718	0.0136	0.2973	0.0362	0.0313
	2.0	0.5	2.0558	0.5053	0.5016	0.0558	0.0053	0.0016	0.1321	0.0003	0.0003
	2.0	0.7	2.0688	0.7222	0.5033	0.0688	0.0222	0.0033	0.2327	0.0010	0.0005
	2.0	0.9	2.0790	0.9729	0.5126	0.0790	0.0729	0.0126	0.3669	0.0366	0.0315

Figur e 4 pr esents the plots of the fitted PDFs (see Figur e 4, Fitted PDFs) and the estimated CDFs (see Figur e 4, estimated CDFs), which equally illustrate that the IWW3 model has fitted the data well compar e to the other competing models. Mor eover, Figur e 4 (estimated hazar d rate function) has indicated that the hazar d rate function is bathtub shaped, and hence, has ascertained the actual beha vior of the data.

Table 4: *MLEs and their standard errors (in parentheses) for the models fitted to the Aarset data.*

Models	$\hat{\eta}$	$\hat{\varphi}$	$\hat{\tau}$	$\hat{\theta}$	$\hat{a}$
EW	0.0109	4.6713	0.1450		
	(0.0009)	(0.0246)	(0.0217)		
WE	0.1742	0.3851	0.0778		
	(0.0621)	(0.1029)	(0.0257)		
W	0.9488	44.847			
	(0.1196)	(6.9313)			
WW	0.2705	0.2558	0.0066		
	(0.0700)	(0.0584)	(0.0059)	1.6026	
NW-W	0.4929	0.0021	1.4560	(0.2263)	
	(0.0893)	(0.0004)	(0.0690)		
IWW3	5.4238	0.1363	61.067		
	(0.0040)	(0.0230)	(3.6212)		

Table 5: *The values of $\ell(\hat{\Psi})$, AIC, CAIC, BIC, K-S(with its p-value) statistics for the models fitted to the Aarset data.*

Models	$-\ell(\hat{\Psi})$	AIC	CAIC	BIC	K-S	p-value
EW	229.136	464.272	464.7937	470.008	0.2057	0.0291
WE	225.6185	457.2371	457.7588	462.9731	0.1289	0.3774
W	241.0019	486.0037	486.259	489.8278	0.1933	0.0477
WW	220.902	449.804	450.6929	457.4521	0.1308	0.3598
NW-W	230.2974	466.5948	467.1166	472.3309	0.2040	0.0312
IWW3	218.3491	442.6982	443.2199	448.4342	0.1192	0.4762

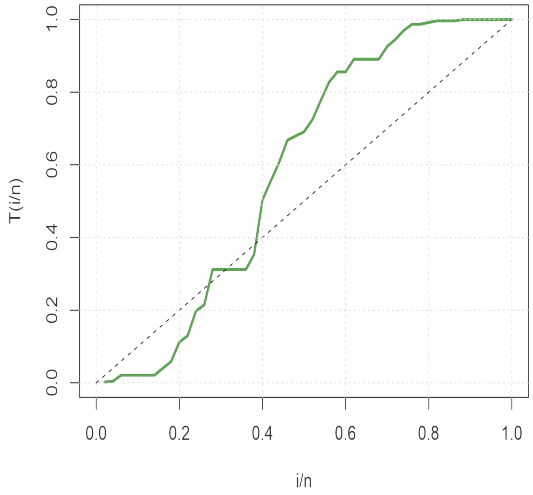

Figure 3: *TTT plot for Aarset data*

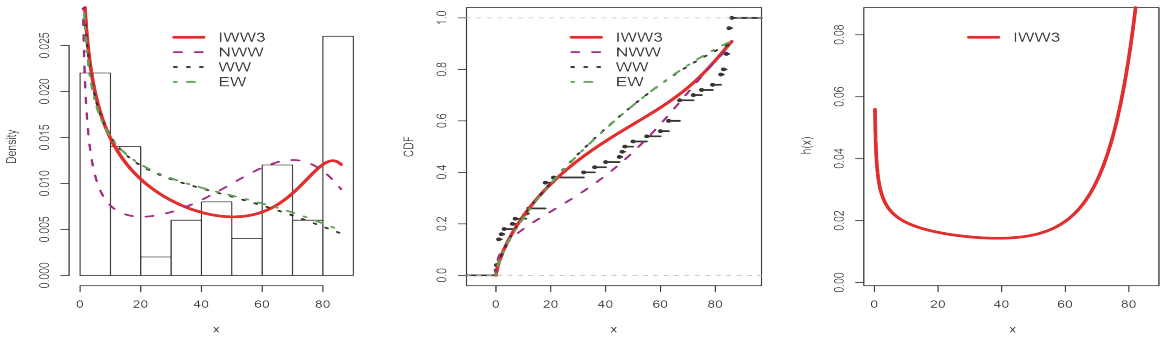

Figure 4: *Fitted PDFs (left panel), estimated CDFs (center panel) and estimated hazard rate function (right panel) for some of the fitted models to Aarset data.*

6.2. Meeker and Escobar data

The second data used is [19] data, which represents the failure and running times of $n = 30$ devices. It has been analyzed by many authors, including [24]. The data revealed a bathtub-shaped FR, as shown by the TTT-plot in Figure 5. Table 6 lists the MLEs of the parameters of IWW3(Ψ) together with that of EW, WE, W, WW, and NW-W for the data. From Table 7, it is note that the IWW3(Ψ) has the smallest $-\ell(\hat{\Psi})$, AIC, CAIC, and BIC values, thus, the IWW3 model provide a better fit for the data. For the formal non-parametric goodness-of-fit statistic, the IWW3 model has the smallest value for K-S, with the highest p-value, which also ascertains the IWW3 model well fits the Meeker and Escoba data.

Figure 6 presents the plots of the fitted PDFs (see Figure 6, Fitted PDFs) and the estimated CDFs (see Figure 6, estimated CDFs), which illustrate that the IWW3 model has fitted the data well

compar e to the other competing models. Additionally , Figur e 6 (estimated hazar d rate function) has indicated that the hazar d rate function is bathtub shaped, and hence, has ascertained the actual beha vior of the data.

Table 6: *MLEs and their standard errors (in parentheses) for the models fitted to the Meeker and Escobar data.*

Models	$\hat{\eta}$	$\hat{\varphi}$	$\hat{\tau}$	$\hat{\theta}$	$\hat{a}$
EW	0.0030	5.5320	0.1620		0.5886
	(0.0002)	(0.2077)	(0.0319)		(0.1375)
WE	0.1258	0.4976	0.0187		
	(0.0669)	(0.2022)	(0.0093)		
W	1.2550	180.652			
	(0.2043)	(26.8740)			
WW	0.0860	0.4936	0.0539		
	(0.0409)	(0.1760)	(0.0304)	0.8357	
NW-W	0.8785	0.0020	1.0669	(0.1147)	
	(0.1653)	(0.0003)	(0.0371)		
IWW3	6.9601	0.1479	239.38		
	(0.0085)	(0.0297)	(14.149)		

Table 7: *The values of $\ell(\hat{\Psi})$, AIC, CAIC, BIC, K-S(with its p-value) statistics for the models fitted to the Meeker and Escobar data.*

Models	$-\ell(\hat{\Psi})$	AIC	CAIC	BIC	K-S	p-value
EW	177.9146	361.8293	362.7524	366.0329	0.2159	0.1219
WE	177.1573	360.3145	361.2376	364.5181	0.1724	0.3347
W	184.35	372.6999	373.1443	375.5023	0.2358	0.0712
WW	178.0157	364.0313	365.6313	369.6361	0.1650	0.3873
NW-W	180.3075	366.6149	367.538	370.8185	0.2234	0.1001
IWW3	170.804	347.608	348.5311	351.8116	0.1425	0.576

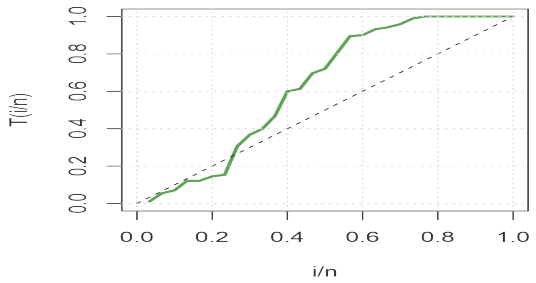

Figure 5: *TTT plot for Meeker and Escoba data.*

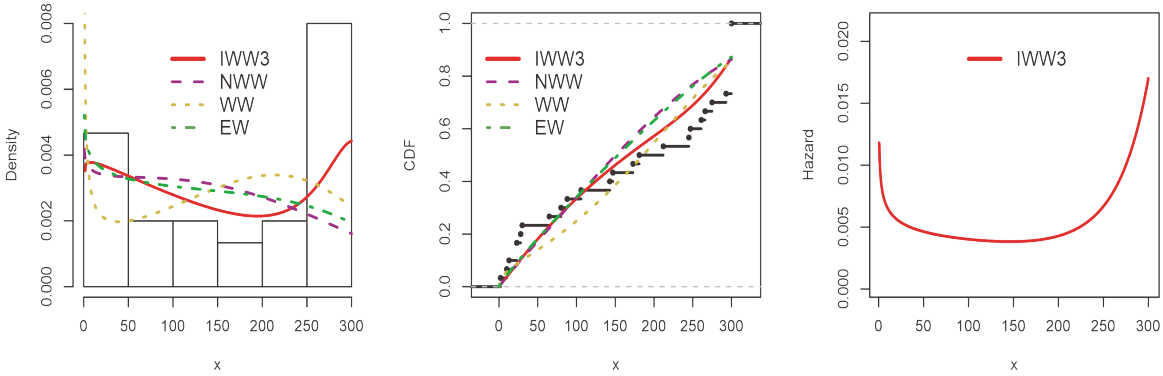

Figure 6: *Fitted PDFs (left panel), estimated CDFs (center panel) and estimated hazard rate function (right panel) for some of the fitted models to Meeker and Escoba data.*

7. Conclusion

This paper defined and studied a new generalized Weibull distribution called the Improved Weibull-Weibull (IWW3) distribution. It is a three-parameter flexible distribution with the ability to accommodates monotone and non-monotone failure rates lifetime data. We obtain explicit expressions for the moment generating function, moments, quantile function, Rényi entropy, and Mathai-Houbold entropy. Numerical results for median, Rényi entropy, Mathai-Houbold entropy and conduct a Monte Carlo simulation study to obtain some numerical results for the mean, variance, skewness, and kurtosis of the distribution. We also characterize the IWW3 model based on two truncated moments and in terms of the hazard function. Estimation of the distribution parameters is performed using the method of maximum likelihood, and the estimation method is assessed by Monte Carlo simulation experiments which yield consistent estimates in the samples considered. Two failure time data having non-monotone failure rate functions are analyzed to demonstrate the potentiality of the distribution.

Disclosure statement
On behalf of The authors, I declare that no potential conflict of interest was reported.
Funding
No funding was provided for the work.

References

[1] Jiang, H., Xie, M., & Tang, L. C. (2008). On the odd Weibull distribution. *Proceedings of the Institution of Mechanical Engineers, Part O: Journal of Risk and Reliability*, 222(4), 583-594.
[2] Souloukngа, M. H., Doka, S. Y., Revanna, N., Djongyang, N., & Kofane, T. C. (2018). Analysis of wind speed data and wind energy potential in Faya-Largeau, Chad, using Weibull distribution. *Renewable energy*, 121, 1-8.
[3] Bayat, H., Rastgo, M., Zadeh, M. M., & Vereecken, H. (2015). Particle size distribution models, their characteristics and fitting capability. *Journal of hydrology*, 529, 872-889.
[4] Wang, Y., & Peng, Z. (2020). Fatigue life prediction method of mechanical parts based on Weibull distribution. *In IOP Conference Series: Materials Science and Engineering*, 782 (2) p. 022068.
[5] Dey, S., Sharma, V. K., & Mesfioui, M. (2017). A new extension of Weibull distribution with application to lifetime data. *Annals of Data Science*, 4, 31-61.
[6] Mudholkar, G. S., & Srivastava, D. K. (1993). Exponentiated Weibull family for analyzing bathtub failure-rate data. *IEEE transactions on reliability*, 42(2), 299-302.
[7] Lai, C. D., Xie, M., & Murthy, D. N. P. (2003). A modified Weibull distribution. *IEEE Transactions on reliability*, 52(1), 33-37.

[8] Coora y, K. (2006). Generalization of the Weibull distribution: the odd Weibull family. *Statistical Modelling*, 6(3), 265-277.
[9] Silv a, G. O., Ortega, E. M., & Cor deir o, G. M. (2010). The beta modified Weibull distribution. *Lifetime data analysis*, 16, 409-430.
[10] Bour guignon, M., Silv a, R. B., & Cor deir o, G. M. (2014). The Weibull-G family of probability distributions. *Journal of data science*, 12(1), 53-68.
[11] Oguntunde, P. E., Balogun, O. S., Okagbue, H. I., & Bishop, S. A. (2015). The Weibull-exponential distribution: Its properties and applications. *Journal of Applied Sciences*, 15(11), 1305-1311.
[12] Tahir, M. H., Cor deir o, G. M., Alizadeh, M., Mansoor, M., Zubair, M., & Hamedani, G. G. (2015). The odd generalized exponential family of distributions with applications. *Journal of Statistical Distributions and Applications*, 2, 1-28.
[13] Ahmad, Z., Elgar hy, M., & Hamedani, G. G. (2018). A new Weibull-X family of distributions: properties, characterizations and applications. *Journal of Statistical Distributions and Applications*, 5, 1-18.
[14] Abd EL-Baset, A. A., & Ghazal, M. G. M. (2020). Exponentiated additiv e Weibull distribution. *Reliability Engineering & System Safety*, 193, 106663.
[15] Mohammed, A. S., & Ugwuo wo, F. I. (2021). On Transmuted Exponential-T opp Leon Distribution with Monotonic and Non-Monotonic Hazar d Rates and its Applications. *Reliability: Theory & Applications*, 16(4 (65)), 197-209.
[16] Mohammed, A. S., & Ugwuo wo, F. I. (2020). A new Four-Parameter Weibull Distribution with Application to Failur e Time Data. *FUDMA Journal of Sciences*, 4(3), 563-575.
[17] Abba, B., Wang, H., & Bakouch, H. S. (2022). A reliability and sur viv al model for one and tw o failur e modes system with applications to complete and censor ed datasets. *Reliability Engineering & System Safety*, 223, 108460.
[18] Wang, H., Abba, B., & Pan, J. (2022). Classical and Bayesian estimations of impr oved Weibull-Weibull distribution for complete and censor ed failur e times data. *Applied Stochastic Models in Business and Industry*, 38(6), 997-1018.
[19] Meeker, W. Q., Escobar, L. A., & Pascual, F. G. (2022). Statistical methods for reliability data. *John Wiley & Sons.*
[20] Cor deir o, G. M., Ortega, E. M., & Lemonte, A. J. (2014). The exponential-W eibull lifetime distribution. *Journal of Statistical Computation and simulation*, 84(12), 2592-2606.
[21] Bakouch, H. S., & Abd El-Bar, A. M. (2017). The exponential-W eibull lifetime distribution. *Journal of Statistical Computation and simulation*, 84(12), 2592-2606.
[22] Glanzel, W. (1987). A characterization theor em based on truncated moments and its application to some distribution families. *In Mathematical Statistics and Probability Theory: Volume B Statistical Inference and Methods Proceedings of the 6th Pannonian Symposium on Mathematical Statistics, Bad Tatzmannsdorf, Austria*, , September 14-20, 1986 (pp. 75-84). Springer Netherlands.
[23] Aarset, M. V. (1987). How to identify a bathtub hazar d rate. *IEEE transactions on reliability*, 36(1), 106-108.
[24] Sar han, A. M., & Apaloo, J. (2013). Expon entiated modified Weibull extension distribution. *Reliability Engineering & System Safety*, 112, 137-144.